ISSN 1831-9424

Results of time-of-flight transmission measurements for ^{209}Bi at a 50 m station of GELINA

Romojaro, P., Paradela Dobarro, C., Alaerts, G., Fiorito, L., Heyse, J., Kopecky, S., Moscati, S., Schillebeeckx, P., Stankovskiy, A., Van Den Eynde, G., Vendelbo, D., Wynants, R.

2024

Joint
Research
Centre

EUR 31873 EN

EU Science Hub

JRC136373

EUR 31873 EN

PDF ISBN 978-92-68-13138-1 ISSN 1831-9424 doi:10.2760/02812 KJ-NA-31-873-EN-N

Luxembourg: Publications Office of the European Union, 2024

How to cite this report: European Commission, Joint Research Centre, Romojaro, P., Paradela Dobarro, C., Alaerts, G., Fiorito, L., Heyse, J., Kopecky, S., Moscati, S., Schillebeeckx, P., Stankovskiy, A., Van Den Eynde, G., Vendelbo, D. and Wynants, R., *Results of time-of-flight transmission measurements for ^{209}Bi at a 50 m station of GELINA*, Publications Office of the European Union, Luxembourg, 2024, https://data.europa.eu/doi/10.2760/02812, JRC136373.

Contents

Abstract 2

Acknowledgements 3

1 Introduction 4

2 Experimental conditions 5

3 Data reduction 7

3.1 Experimental transmission 7

3.2 Background correction 7

4 Results and comparison with nuclear data libraries 10

5 Summary and conclusions 16

References 17

List of abbreviations and definitions 19

List of figures 20

List of tables 21

Annexes 22

Annex 1. Summary of the experiment information 22

Annex 2. Summary of data format 25

Annex references 27

Abstract

Transmission measurements through metallic bismuth samples have been performed at the time-of-flight facility GELINA. The measurements have been carried out at a 50 m transmission station using a Li-glass scintillator with the accelerator operating at 400 Hz. This report provides the experimental details required to deliver the data to the EXFOR data library which is maintained by the International Network of Nuclear Reaction Data Centres (NRDC). The experimental conditions and data reduction procedures are described. In addition, the full covariance information based on the AGS concept is given, such that nuclear reaction model parameters together with their covariances can be derived in a least-squares adjustment to the data. The experimental transmissions were used to verify the resonance parameters in the main evaluated nuclear data libraries. Recommendations to improve the parameters in the resolved resonance region are given.

Acknowledgements

The experiment was carried out under the Research Infrastructure Access Agreement N° 35543/1/2019-1-RD-EUFRAT-GELINA. This work received funding from the Euratom research and training programme 2014-2018 under Grant Agreement Number 847552 (SANDA Project).

Authors

Pablo Romojaro

Carlos Paradela Dobarro

Gery Alaerts

Luca Fiorito

Jan Heyse

Stefan Kopecky

Sandro Moscati

Peter Schillebeeckx

Alexey Stankovskiy

Gerd Van Den Eynde

Danny Vendelbo

Ruud Wynants

1 Introduction

To study the resonance structure of neutron induced reaction cross sections, neutron spectroscopic measurements are required, which determine with high accuracy the energy of the neutron that interacts with the material under investigation. To cover a broad energy range, such measurements are best carried out with a pulsed white neutron source, which is optimized for time-of-flight (TOF) measurements [1].

The TOF-facility GELINA [2,3] has been designed and built for high-resolution cross section measurements in the resonance region. It is a multi-user facility, providing a white neutron source with a neutron energy range from 10 meV to 20 MeV. The GELINA facility can host experiments at measurement stations located between 10 m and 400 m from the neutron production target. The electron linear accelerator provides a pulsed electron beam with a maximum energy of 150 MeV, a maximum peak current of 10 A and a repetition rate ranging from 50 Hz to 800 Hz. A compression magnet reduces the width of the electron pulses to about 2 ns [4]. The electron beam hits a mercury-cooled uranium target producing Bremsstrahlung and subsequently neutrons via photonuclear reactions [5]. Two water-filled beryllium containers mounted above and below the neutron production target are used to moderate the neutrons. By applying different neutron beam collimation conditions, experiments can use either a fast or a moderated neutron spectrum. The neutron production rate is monitored by BF_3 proportional counters which are mounted in the ceiling of the target hall. The output of the monitors is used to normalize the time-of-flight spectra to the same neutron intensity. The measurement stations are equipped with air conditioning systems to reduce electronic drifts in the detection chains due to temperature changes. The temperature in the measurement stations is continuously monitored.

This report describes the transmission measurements carried out at GELINA with natural bismuth metallic discs of 1.255 mm and 4 mm thickness. The measurements were carried out within the framework of the Horizon 2020 Euratom research and training program under grant agreement No 847552 (SANDA) [6] and within the EUFRAT open access program, i.e. project “Bismuth_MYRRHA”. The report provides the information required for extracting resonance parameters by a resonance shape analysis using a code such as REFIT [7]. In the description of the data, the recommendations resulting from a consultant’s meeting organized by the Nuclear Data Section of the IAEA (NDS/IAEA) have been followed [8].

2 Experimental conditions

The transmission experiments were performed at the 50 m measurement station of flight path 4 with the accelerator operating at 400 Hz. The moderated neutron spectrum was used. A shadow bar made of Cu and Pb was placed close to the uranium target to reduce the intensity of the γ-ray flash and the fast neutron component. The flight path forms an angle of 9° with the direction normal to the face of the moderator viewing the flight path. The samples and detector were placed in an acclimatized room to keep them at a temperature of about 20°C. A schematic view of the experimental set-up is shown in Figure 1.

Figure 1. Schematic representation of the transmission set-up at the 50 m station of GELINA.

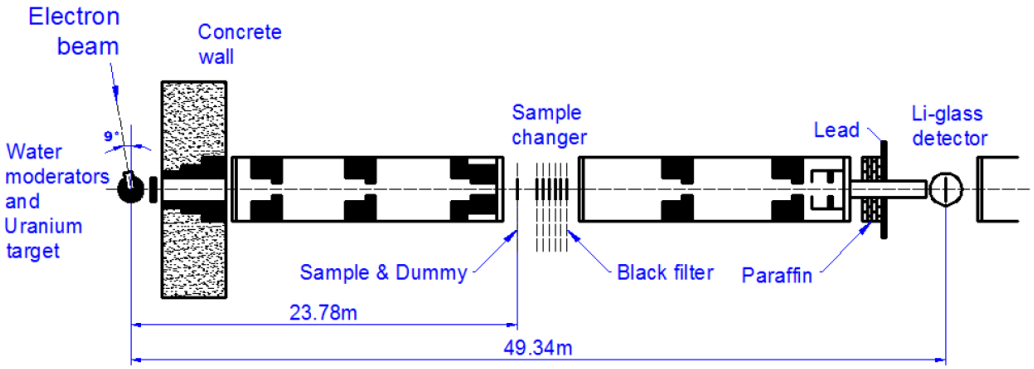

The neutrons scattered from the moderator were collimated into the flight path through an evacuated aluminum pipe of 50 cm diameter with annular collimators, consisting of borated wax, copper and lead. A set of Pb, Ni and Cu annular collimators was used to reduce the neutron beam to a diameter of 45 mm at the sample position. Additional lithium and B_4C collimators were installed to absorb neutrons that are scattered by the collimators. A ^{10}B overlap filter with an areal density of about 0.08 at/b was placed close to the neutron target to minimize the contribution of slow neutrons coming from previous accelerator bursts. The impact of γ-rays in the neutron detector was reduced by a 16 mm thick Pb filter.

The sample and back resonance filters were placed in independent and automatic sample changers at a distance of approximately 24 m from the neutron source. The neutron beam passing through the sample and filters was further collimated and detected by a 6.35 mm x 151.6 mm diameter NE912 Li-glass scintillator. The scintillator is connected through a boron-free quartz window to a 127 mm EMI 9823 KQB photomultiplier (PMT), which was placed outside the neutron beam perpendicular to its axis. The detector was placed at about 47 m from the neutron target and the diameter of the neutron beam at the detector position was about 90 mm.

Sodium, cobalt and tungsten black resonance filters were mounted in the sample changers to determine the background contribution at 2850 eV, 132 eV and 18 eV, respectively, and to obtain its time dependence. The cobalt and the tungsten filters were inserted permanently in the beam to continuously monitor the background level and to account for the impact of the sample or filters placed in the beam [1].

The processing of the time and amplitude signals was based on analog electronics [9]. The TOF of the detected neutrons was derived from the time difference between the stop signal T_s, obtained from

the anode pulse of the PMT, and the start signal T_0, given at each electron burst. This time difference was processed with a multi-hit fast time coder with a 1 ns time resolution. The TOF and the pulse height of each detected event were recorded in list mode using a multi-parameter data acquisition system developed at the EC-JRC. Each measurement was subdivided in different cycles. Only cycles for which the ratio between the total counts in the transmission detector and in the neutron monitor deviated by less than 1% were selected.

The dead time of the detection chain t_d = 3300 (10) ns was derived from a spectrum of the time-interval between successive events. The maximum dead time correction was less than 20% for energies below 100 keV. In Ref. [1], it is demonstrated that uncertainties for such dead time corrections are very small and can be neglected.

The measurements were performed with metallic discs composed of high purity (99.9999%) natural bismuth. Two samples of 1.255 mm and 4 mm thickness were prepared. The area was determined by an optical surface inspection with a microscope system from Mitutoyo. The main characteristics of the samples are reported in Table 1.

Table 1. Characteristics of the bismuth samples used for the transmission measurements. The areal densities n_d were derived from the measured mass and area and the ^{209}Bi atomic mass reported in Ref. [10].

Sample	Thickness / mm	Mass / g	Area / mm^2	Areal Density / (at/b)
NS05009	4	201.865 (10)	5256 (5)	1.1066 (11) x 10^{-2}
NS05024	1.255	62.214 (10)	5147 (5)	3.483 (4) x 10^{-3}

3 Data reduction

The AGS code [11,12] developed at the JRC Geel, was used to derive the experimental transmission from the TOF-spectra. The code is based on a compact formalism to propagate both the correlated and uncorrelated uncertainties starting from uncorrelated uncertainties due to counting statistics.

3.1 Experimental transmission

The experimental transmission T_{exp} as a function of TOF was obtained from the ratio of a sample-in measurement C_{in} and a sample-out measurement C_{out}, both corrected for their background contributions B_{in} and B_{out}, respectively:

$$T_{exp} = N\frac{C_{in} - KB_{in}}{C_{out} - KB_{out}}. \quad (3.1)$$

The factor N accounts for uncertainties due to variations in the beam intensity and K for systematic effects due to the background model. The TOF spectra, C_{in} and C_{out}, were corrected for losses due to the dead time in the detector and electronics chain. All spectra were normalized to the same TOF-bin width structure and neutron beam intensity. The latter was derived from the response of the BF_3 beam monitors. To avoid systematic effects due to slow variations of both the beam intensity and detector efficiency as a function of time, data were taken by alternating sample-in and sample-out measurements in cycles of about 600 seconds. Such a procedure reduces the uncertainty on the normalization to the beam intensity to less than 0.25%. This uncertainty was evaluated from the ratios of counts in the ^{6}Li transmission detector and in the flux monitors. To account for this uncertainty the factor N = 1.0000 (25) was introduced in Eq. (3.1). The background as a function of TOF was approximated by an analytic expression applying the black resonance technique [1]. The factor K = 1.00 (3) in Eq. (3.1) was derived from a statistical analysis of the difference between the observed black resonance dips and the estimated background [14]. This uncertainty is only valid for measurements with at least two fixed black resonance filters in the beam [1].

The time-of-flight (t) of a neutron creating a signal in the neutron detector was determined by the time difference between the stop signal (T_s) and the start signal (T_0):

$$t = (T_s - T_0) + t_0, \quad (3.2)$$

with t_0 a time-offset which was determined by a measurement of the γ-ray flash. The flight path distance L = 47.669 (4) m, i.e. the distance between the centre of the moderator viewing the flight path and the front face of the detector, was derived previously from results of transmission measurements using a uranium sample and the resonance energies for ^{238}U+n reported by Derrien et al. [14].

3.2 Background correction

The background contribution for the transmission measurements was approximated by an analytical function, consisting of the sum of a time-independent and three time-dependent components:

$$B(t) = b_0 + b_1 e^{-\lambda_1 t} + b_2 e^{-\lambda_2 t} + b_3 e^{-\lambda_3 (t+\tau_0)} \quad (3.3)$$

The time independent component b_0 is related to the ambient radiation and background contributions that lost any time correlation. The first time-dependent component is due to 2.2 MeV γ-rays resulting from neutron capture in hydrogen present in the moderator. The second exponential term originates predominantly from neutrons scattered inside the detector station. The last component is attributable to slow neutrons, with energies below 2 eV, from previous accelerator cycles. This contribution was estimated by an extrapolation of the TOF-spectrum at the end of the cycle. The time shift τ_0 is the inverse of the accelerator frequency, i.e. τ_0 = 2.5 ms for 400 Hz. The other terms of the analytical function were obtained applying the black resonance technique [1]. The time dependence of the first and the second time-dependent background components was studied by including short cycles with Na, Co and W filters in the beam. The decay constants λ_1 and λ_2 were previously derived from results of measurements including additional black resonance filters such as S and Ag or a polyethylene filter. Permanent Co and W filters were placed in the beam to monitor continuously the background level and the sample presence. Example of a dead-time corrected and normalized sample-in spectrum with the background contributions from Eq. (3.3) is shown in Figure 2 for the 1.255 mm sample. Parameters for the analytical expressions of the background correction for the 1.255 mm and 4 mm sample-in and sample-out measurements are presented in Table 2 and Table 3, respectively. The uncertainties of the parameters resulting from propagating uncertainties due to counting statistics are not given. Their impact on the final uncertainty of the transmission is negligible compared to the 3% uncertainty due to the model.

Figure 2. TOF-spectrum resulting from measurements with the ^{209}Bi 1.255 mm sample with Co and W black resonance filters in the beam and the accelerator operated at 400 Hz. The sample-in spectrum (C_{in}) is shown together with the total background (B_{in}) and its components defined in Eq. (3.3).

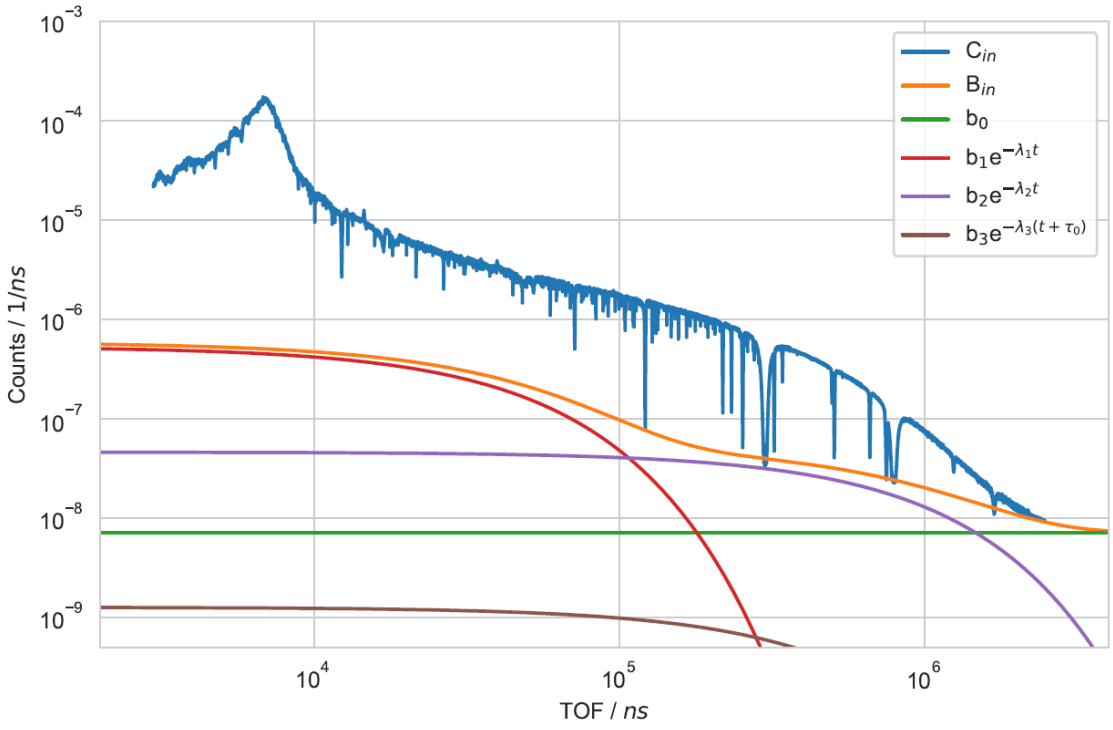

Table 2. Parameters for the analytical expressions of the background correction for the 1.255 mm sample-in and sample-out measurements. The parameters are derived from results of measurements with the Co and W black resonance filters in the beam and the accelerator operating at 400 Hz.

ID	b_0 / 10^{-9}	b_1 / 10^{-7}	$-\lambda_1$ / 10^{-5} ns^{-1}	b_2 / 10^{-8}	$-\lambda_2$ / 10^{-6} ns^{-1}	b_3 / 10^{-7}	$-\lambda_3$ / 10^{-6} ns^{-1}
B_{in}	7.16	5.33	-2.40	4.63	-1.27	6.58	-2.50
B_{out}	7.27	5.49	-2.40	4.86	-1.30	6.76	-2.50

Table 3. Parameters for the analytical expressions of the background correction for the 4 mm sample-in and sample-out measurements. The parameters are derived from results of measurements with the Co and W black resonance filters in the beam and the accelerator operating at 400 Hz.

ID	b_0 / 10^{-9}	b_1 / 10^{-7}	$-\lambda_1$ / 10^{-5} ns^{-1}	b_2 / 10^{-8}	$-\lambda_2$ / 10^{-6} ns^{-1}	b_3 / 10^{-7}	$-\lambda_3$ / 10^{-6} ns^{-1}
B_{in}	6.97	4.76	-2.40	4.57	-1.35	6.12	-2.50
B_{out}	7.27	5.41	-2.40	5.00	-1.35	6.76	-2.50

4 Results and comparison with nuclear data libraries

The AGS code [11,12] was used to derive the experimental transmission and propagate both the correlated and uncorrelated uncertainties. The code is based on a compact formalism to propagate all uncertainties starting from uncorrelated uncertainties due to counting statistics. It stores the full covariance information after each operation in a concise, vectorized way. The AGS formalism results in a substantial reduction of data storage volume and provides a convenient structure to verify the various sources of uncertainties through each step of the data reduction process. The concept is recommended by the NDS/IAEA [8] to prepare the experimental observables, including their full covariance information, for storage into the EXFOR data library [15,16].

The format in which the numerical data will be stored in the EXFOR data library is illustrated in Annex 2. The data include the full covariance information based on the AGS concept. The total uncertainty and the uncertainty due to uncorrelated components are reported, together with the contributions due to the normalization and background subtraction. Applying the AGS concept the covariance matrix V of the experimental transmission can be calculated by:

$$V = U_u + S(\eta)S(\eta)^T, \tag{4.1}$$

where U_u is a diagonal matrix containing the contribution of all uncorrelated uncertainty components. The matrix S contains the contribution of the components η = {N, K} creating correlated components. The uncertainty due to the dead time correction can be neglected. The experimental details, which are required to perform a resonance analysis on the data, are summarized in the Annex 1.

The experimental transmissions presented in this work were used to verify recommended resonance parameters for neutron interactions with ^{209}Bi. The basis of the resonance parameters in the main nuclear data libraries (ENDF, JEFF, JENDL) is the compilation of Mughabgahb et al. published in 1984 [17]. The parameters of the 2006 compilation [18], which includes the results of the capture measurements at GELINA by Mutti [19], are not used in the main libraries. The origin of the parameters of the 1984 compilation is not traceable. Most probably, they are a combination of parameters resulting from transmission experiments reported by Morgenstern et al. [20], Singh et al. [21] and Musgrove and Harvey [22], and the capture kernels obtained from the capture measurements of Macklin and Halperin [23]. In any case they are not the result of a combined resonance shape analysis of experimental cross section data (transmissions and capture yields) reported in the literature.

Although the headers of the libraries do not provide detailed information about the construction of the resonance parameter files in ENDF/B-VIII.0, JENDL-4.0, JENDL-5 and JEFF-3.3, we will try to summarize their origin. For these libraries there is only a separation between resolved resonance region and continuum. No unresolved resonance region with average resonance parameters is included.

The parameters of Mughabghab et al. [17] of 1984 are adopted in the ENDF/B-VIII.0 library. The file does not include a negative resonance and the resolved resonance region goes up to 100 keV. Between 100 keV and 1.92 MeV a structured point wise cross section is given, which was (most probably) derived from the high resolution cross section data of Harvey [24].

The parameters of Mughabghab et al. [17] are the basis for JENDL-4.0, with a resolved resonance region that extends to 200 keV. The parameters for energies below 24 keV were replaced by those of Domingo-Pardo et al. [25], which were derived from an analysis of capture cross section data at the n_TOF facility. The results of capture cross section measurements at GELINA reported by Mutti

[19], which extend to 80 keV, were not considered. Between 100 keV and 200 keV only s-wave resonances are included. A negative resonance is added together with a negative point wise total cross section (file 3) between 30 keV and 200 keV. Between 200 keV and 2 MeV a structured total cross section based on the results of Refs. [26,27,28} is given. This cross section is derived from experimental data with a lower energy resolution compared to the data used for the cross section in ENDF/B-VIII.0. The cross section in JENDL-4.0, including the negative resonance and background cross section, is taken over in JEFF-3.3. In the JENDL-5 library only the resonance parameters of JENDL-4.0, without the additional negative point wise cross section, are adopted. In addition, the total cross section in JENDL-5 above 200 keV differs from JENDL-4.0. It follows, like ENDF/B-VIII.0, the cross section of Harvey without making any reference to this work.

To verify the resonance parameters in the ENDF/B-VIII.0, JENDL-4.0 and JENDL-5 libraries the experimental transmissions are compared with the calculated ones using the parameters in these libraries. For energies below 200 keV (100 keV for ENDF/B-VIII.0) the calculated transmission $T_M(t)$ is derived with the REFIT code [7]:

$$T_M(t) = \int R(t,E) e^{-n\,\overline{\sigma_{tot}}}\, dE \qquad (4.2)$$

with $\overline{\sigma_{tot}}$ the energy dependent Doppler broadened total cross section, n the areal density of the sample and R(t,E) the response function of GELINA. For a better interpretation of the data the time of flight was transferred into neutron energy using the same fixed flight path length for the experimental and calculated data.

Figure 3. Comparison of the experimental and calculated transmission through the 1.255 mm thick Bi sample. The calculated transmissions are obtained with REFIT using the resonance parameters in JENDL-4.0 and ENDF/B-VIII.0, including a neutron energy adjustment to match the experimental result.

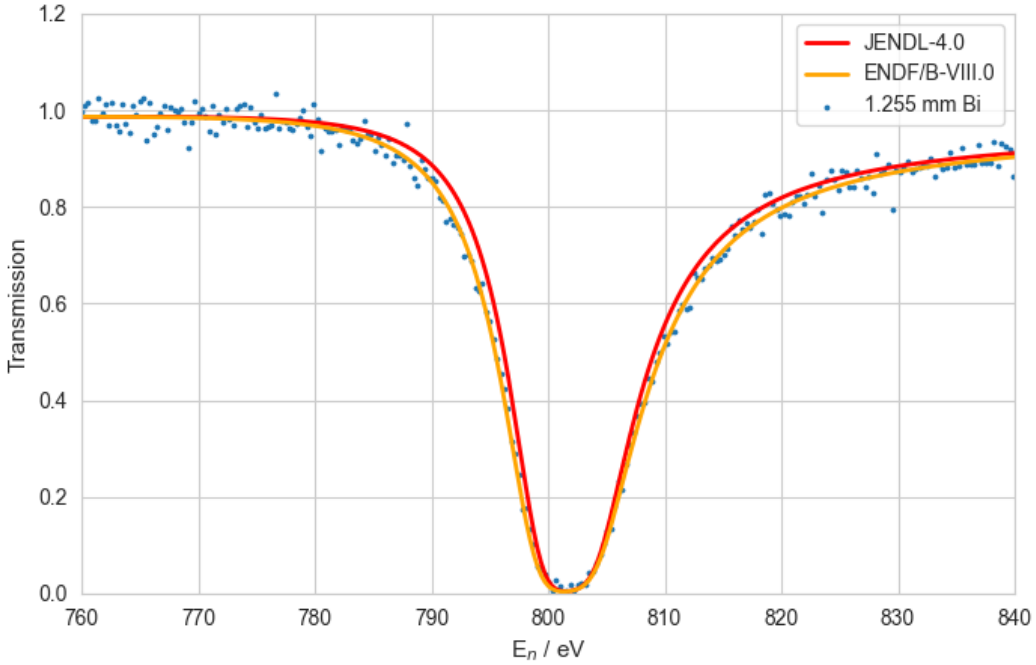

The resonance energies in the libraries are not fully consistent with the data derived at GELINA and there is also some inconsistency between resonance energies adopted in different libraries. This can be solved by including the data presented in this work in a new evaluation which would make the resonance energies traceable to the energies of ^{238}U resonances derived by Derrien et al. [14]. Figure 3 shows the transmission through a 1.255 mm thick Bi sample in the region of the strong s-wave resonance at 800 eV. It compares the experimental transmission with the theoretical transmission derived from the resonance parameters in JENDL-4.0 and ENDF/B-VIII.0. For a better representation of the data the neutron energies were adjusted. The calculated transmission obtained with the neutron width in ENDF/B-VIII.0, which is derived from the transmission data in Ref. [22], is in much better agreement with the experimental data than the transmission calculated with the one in JENDL-4.0. The latter is adopted from Ref. [25], which is based on the capture data obtained at the n_TOF facility. This shows the shortcomings of deriving neutron widths only from capture yields for a nucleus like ^{209}Bi. For ^{209}Bi, the radiation width is in general much smaller compared to the neutron width such that the neutron width is derived from the resonance profile. This requires an accurate description of the TOF-response function.

The discrepancy between JENDL-4.0 and JENDL-5 for energies above 30 keV, shown in Figure 4, is due to a difference in the background cross section. This negative background cross section, only included in JENDL-4.0, is present for energies up to 200 keV.

Figure 4. Comparison of the experimental and calculated transmission through the 4 mm thick Bi sample for energies between 50 keV and 100 keV. Figure shows the impact of the negative background cross section included in JENDL-4.0, which is not present in JENDL-5.

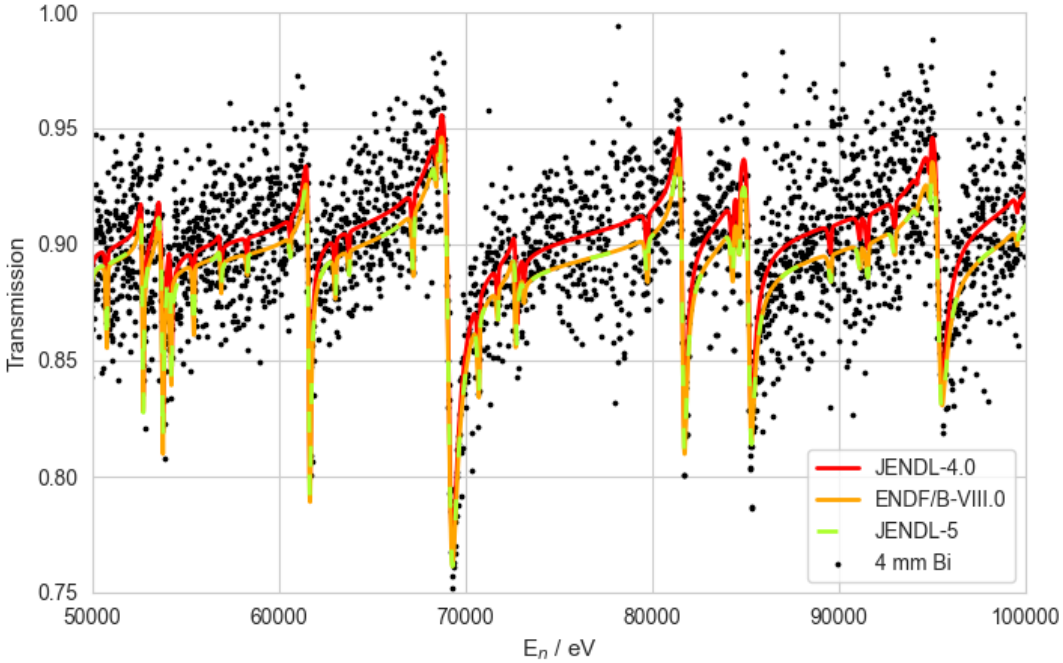

Figure 5 shows the experimental and the calculated transmission for energies between 100 and 150 keV. Above 100 keV, there are no resonance parameters in the ENDF/B-VIII.0 evaluation. The point wise cross section is derived from unpublished transmission data of Harvey [24]. The data that are available in the EXFOR database, are presented as cross sections, which have certainly being obtained from the ratio between the logarithmic of the measured transmission and the areal density of the very thick bismuth sample (0.5651 at/b).

Figure 5. Comparison of experimental and calculated transmission through the 4 mm thick Bi sample for energies between 100 keV and 150 keV.

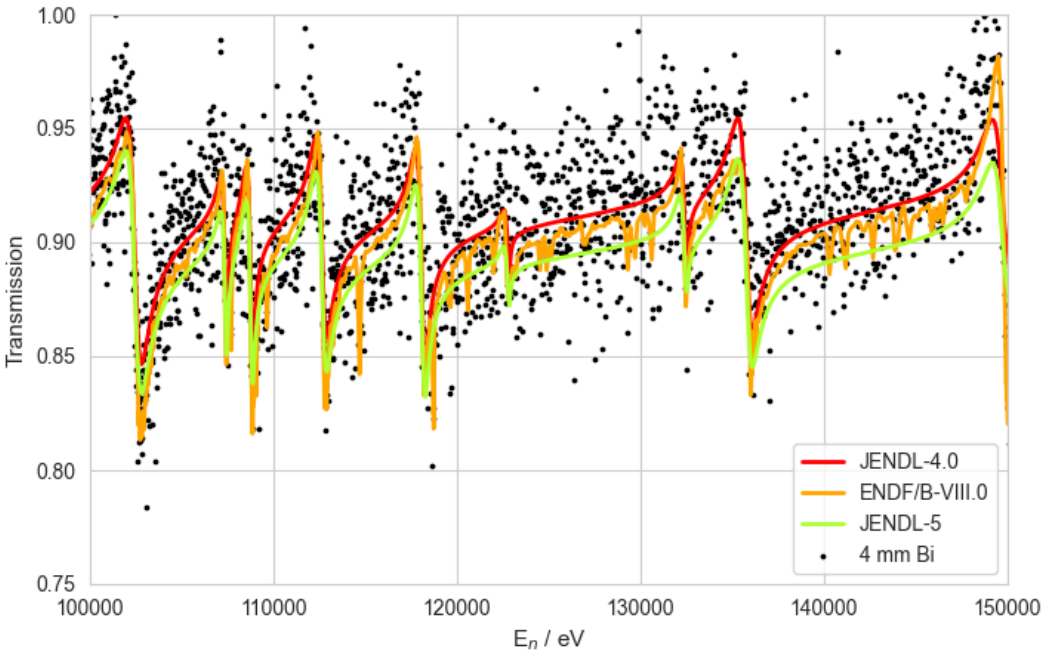

Because the limitations of GELINA data above 150 keV neutron energy, Figures 6 and 7 compare the evaluated cross sections to Harvey's experimental data. The difference in resonance structure is clearly visible. Figures 5 and 6 reveal that by adopting only the resonance parameters of JENDL-4.0 without considering the additional background cross section, the theoretical transmission obtained with JENDL-5 is underestimated and the cross section, overestimated.

Figure 6. Comparison of evaluated cross sections and Harvey's experimental data [24] for energies between 150 keV and 200 keV. It shows that ENDF/B-VIII.0 evaluation follows Harvey's experimental data.

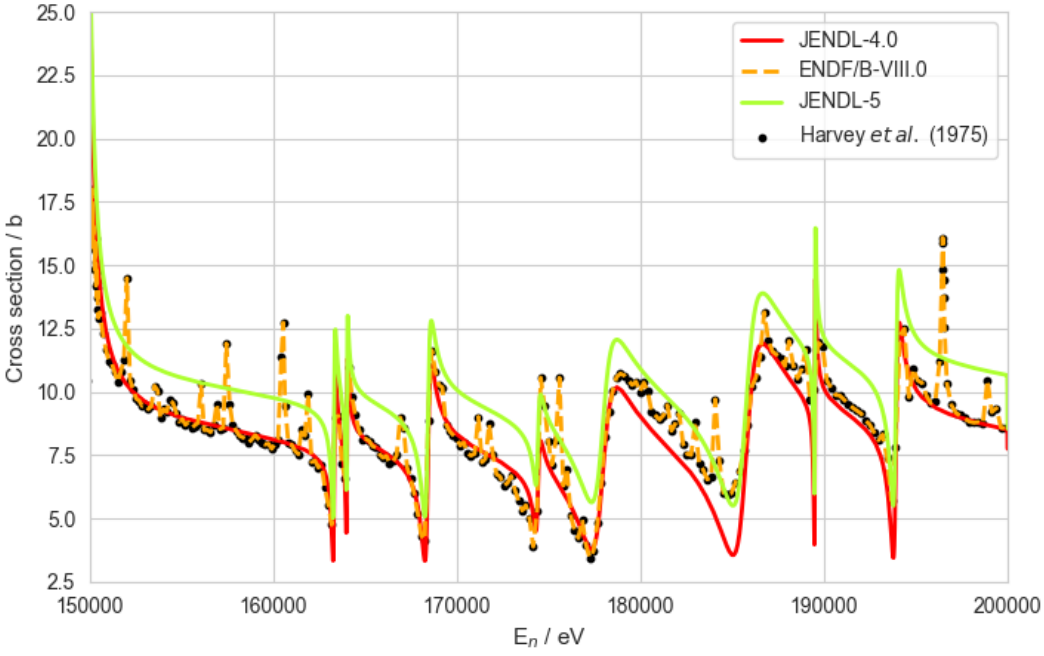

The data in Figure 7 clearly show that JENDL-5 adopted the point wise cross section given in ENDF/B-VIII.0, which exactly reproduces the experimental data from reference [24].

Figure 7. Comparison of evaluated cross sections and Harvey's experimental data for energies between 200 keV and 300 keV. It clearly shows that, above 200 keV, the JENDL-5 evaluation, like ENDF/B-VIII.0, follows Harvey's experimental data.

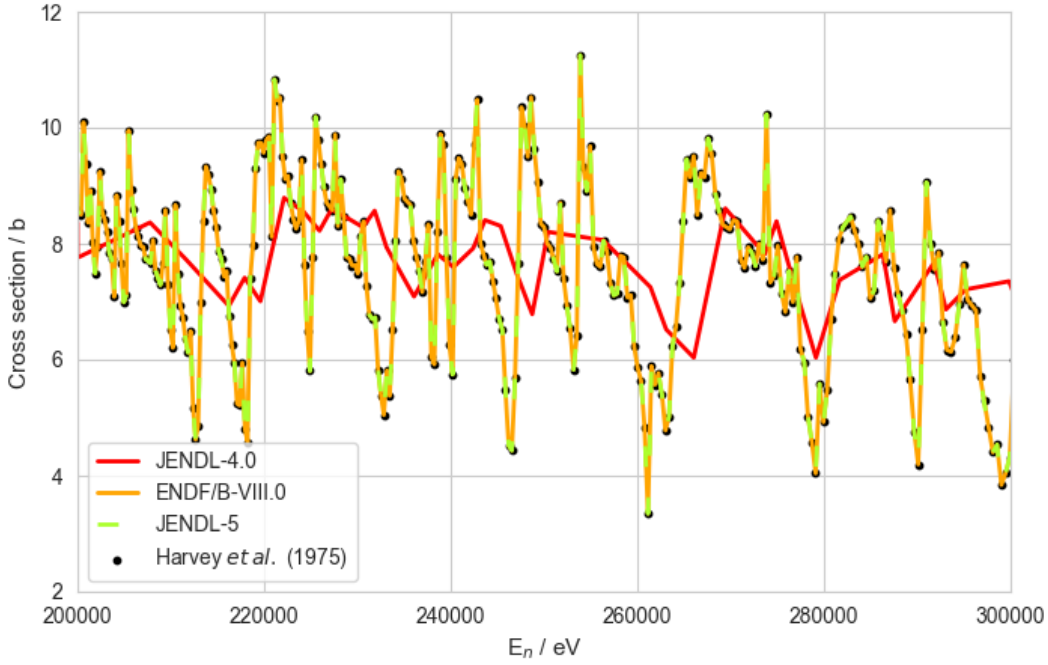

5 Summary and conclusions

This report provides experimental transmission data for a 1.255 and 4 mm thick metallic Bi-samples measured at the GELINA facility. The data were compared with calculated transmissions using the resonance parameters and total cross section data in the JENDL-4.0, JENDL-5 and ENDF/B-VIII.0 libraries. Some differences in the resolved resonance region are due to the inclusion of n_TOF resonance parameters [25] in JENDL-4.0 and JENDL-5 and to the omission of the background cross section in the update of JENDL-5 library. None of the libraries includes an unresolved resonance region.

This comparison reveals that a new evaluation for the cross sections of neutron interactions with ^{209}Bi in the resonance region is required. Such a new evaluation should be based on a resonance shape analysis of the data presented in this work together with the high-resolution transmission data of Harvey [24], the low energy transmission data in Refs. [29, 30, 31, 32] and the capture areas of Mutti [19]. The low energy transmission data include an estimation of the scattering lengths. Unfortunately, there are no capture yields available in EXFOR or in the literature that can be included in such a resonance shape analysis. Therefore, new capture measurements and a reporting of the capture yields are recommended. In addition, the need of a parameterization of the cross section data in terms of average resonance parameters should be verified.

References

1. P. Schillebeeckx, B. Becker, Y. Danon, K. Guber, H. Harada, J. Heyse, A.R. Junghans, S. Kopecky, C. Massimi, M.C. Moxon, N. Otuka, I. Sirakov and K. Volev, "Determination of resonance parameters and their covariances from neutron induced reaction cross section data", Nucl. Data Sheets 113 (2012) 3054 – 3100.

2. A. Bensussan and J.M. Salomé, "GELINA: A modern accelerator for high resolution neutron time of flight experiments", Nucl. Instr. Meth. 155 (1978) 11 – 23.

3. W. Mondelaers and P. Schillebeeckx, "GELINA, a neutron time-of-flight facility for neutron data measurements", Notiziario Neutroni e Luce di Sincrotrone 11 (2006) 19–25. https://web.archive.org/web/20061106054243/http:/www.fisica.uniroma2.it/~notiziario/2006/11_2_06/pag19.pdf (accessed May 19, 2023).

4. D. Tronc, J.M. Salomé and K.H. Böckhoff, "A new pulse compression system for intense relativistic electron beams", Nucl. Instr. Meth. 228 (1985) 217 – 227.

5. J. M. Salome and R. Cools, "Neutron producing targets at GELINA", Nucl. Instr. Meth. 179 (1981) 13 – 19.

6. EC H2020 SANDA project, https://cordis.europa.eu/project/id/847552

7. M. .C. Moxon and J.B. Brisland, Technical Report AEA-INTEC-0630, AEA Technology (1991).

8. F. Gunsing, P. Schillebeeeckx and V. Semkova, "Summary Report of the Consultants' Meeting on EXFOR Data in Resonance Region and Spectrometer Response Function", IAEA Headquarters, Vienna, Austria, 8-10 October 2013, INDC(NDS)-0647 (2013), https://www-nds.iaea.org/index-meeting-crp/CM-RF-2013/ (03/05/2016).

9. C. Paradela Dobarro, J. C. Drohe, J. Heyse, S. Kopecky, S. Moscati, L. Salamon, P. Schillebeeckx, D. Vendelbo and R. Wynants, "Electronic setup for time-of-flight cross section measurements at GELINA", Publications Office of the European Union, Luxembourg, 2021, ISBN 978-92-76-43927-1, doi:10.2760/477469, JRC127003.

10. M.E. Wieser. Atomic Weights of the Elements 2005 (IUPAC Technical Report). Pure Appl. Chem. 78 (2006) 2051-2066.

11. B. Becker, C. Bastian, J. Heyse, S. Kopecky and P. Schillebeeckx, "AGS – Analysis of Geel Spectra User's Manual", NEA/DB/DOC(2014)4.

12. B. Becker, C. Bastian, F. Emiliani, F. Gunsing, J. Heyse, K. Kauwenberghs, S. Kopecky, C. Lampoudis, C. Massimi, N. Otuka, P. Schillebeeckx and I. Sirakov, "Data reduction and uncertainty propagation of time-of-flight spectra with AGS", J. of Instrumentation, 7 (2012) P11002 – 19.

13. I. Sirakov, B. Becker, R. Capote, E. Dupont, S. Kopecky, C. Massimi, and P. Schillebeeckx, "Results of total cross section measurements for 197Au in the neutron energy region from 4 to 108 keV at GELINA", Eur. Phys. J. A 49 (144) (2013) 1.

14. H. Derrien, L.C. Leal, N.M. Larson and A. Courcelle, "Neutron Resonance Parameters of 238U and the Calculated Cross Sections from the Reich-Moore Analysis of Experimental Data in the Neutron Energy Range from 0 keV to 20 keV", Report ORNL/TM-2005/241, Oak Ridge National Laboratory (2005).

15. N. Otuka et al., “Towards a More Complete and Accurate Experimental Nuclear Reacton Data Library (EXFOR): International Collaboration Between Nuclear Reaction Data Centres (NRDC)”, Nucl. Data Sheets 120 (2014) 272-276.

16. N. Otuka, A. Borella, S. Kopecky, C. Lampoudis, and P. Schillebeeckx, “Database for time-of-flight spectra with their covariances”, J. Korean Phys. Soc. 59 (2011) 1314 – 1317.

17. S. F. Mughabghab, “Neutron Cross Sections, Neutron Resonance Parameters and Thermal Cross Sections”, Vol. 1, Part B:Z= 61-100, Academic Press, New York (1984).

18. S. F. Mughabghab, “Atlas of Neutron Resonances. Resonance Parameters and Thermal Cross Sections”, April 2006, Elsevier (5-th edition of BNL-325).

19. P. Mutti, “s-Process implications of ^{136}Ba, ^{208}Pb and ^{209}Bi stellar capture rates”, PhD tesis, Ghent University, 1997.

20. J. Morgensten, R.N. Alves, J. Julien, C. Samour, “Paramètres des résonances et fonctions densités S0 et S1 pour Cl, ^{51}V, ^{89}Y, Zr, La, ^{141}Pr et ^{209}Bi”, Nucl. Phys. A 123 (1969) 561.

21. U. N. Singh, J. Rainwater, H.I. Liou, G. Hacken, “Neutron resonance spectroscopy: ^{209}Bi”, Phys. Rev. C 13 (1976) 124.

22. A. R. de L. Musgrove and J. A. Harvey, “Neutron resonance Spectroscopy on ^{209}Bi”, Australian Journal of Physics 31(1) (1978) 47.

23. R. Macklin and J. Halperin, “Resonance neutron capture by ^{209}Bi”, Phys. Rev. C 14 (1976) 1389.

24. W. Harvey, Oak Ridge National Lab. Reports, No 4743, 54 (1972) and EXFOR entry 13761.

25. C. Domingo-Pardo et al., “New measurements of neutron capture resonances in ^{209}Bi”, Phys. Rev. C 74 (2006) 025807.

26. D. G. Foster Jr. and D. W. Glasgow, “Neutron Total Cross Sections 2.5-15 MeV” , Phys. Rev. C 3 (1971) 576.

27. A. B. Smith, J. F. Whalen, E. Barnard, J. A. M. de Villiers and D. Reitmann,“Fast-Neutron Total and Scattering Cross Sections of Bismuth”, Nucl. Sci. Eng. 41 (1970) 63.

28. S. Cierjacks, P. Forti, D. Kopsch, L. Kropp, J. Nebe and H. Unseld,“High Resolution Total Neutron Cross-Sections between 0.5 and 30 MeV”, Euratom report EUR 3963 (1968).

29. W. Dilg and H. Vonach, “Precise Measurement of the total cross section of bismuth, lead and carbon for 130 eV neutrons”, Zeitschrift fur Naturforschung, Section A, Vol. 26 (1971) 442.

30. L. Koester, W. Waschkowski and J. Meier, “Experimental study on the electric polarizability of the neutron”, Zeitschrift fur Physik A 329 (1988) 229.

31. L. Koester, W. Waschkowski, L.V. Mitsyna, G.S. Samosvat, P. Prokofjevs and J. Tambergs, “Neutron-electron scattering length and electric polarizability of the neutron derived from cross sections of bismuth and of lead and its isotopes”, Physical Review C 51 (1995) 3363.

32. R. E. Mayer, V. H. Gillete and J. R. Granada, “Total Cross Section of Sulphur at Slow Energies”, Zeitschrift fur Naturforschung A 42 (1987) 791.

List of abbreviations and definitions

Abbreviations	Definitions
AGS	Analysis of Geel Spectra
ENDF	Evaluated Nuclear Data File
EUFRAT	European research infrastructure for nuclear reaction, radioactivity, radiation and technology studies in science and applications
EXFOR	EXchange FORmat
GELINA	GEel LINear Accelerator
JEFF	Joint Evaluated Fission and Fussion
JENDL	Japanese Evaluated Nuclear Data Library
MYRRHA	Multi-purpose Hybrid Research Reactor for High-tech Applications
NDS/IAEA	Nuclear Data Section/International Atomic Energy Agency
NRDC	Nuclear Reaction Data Centres
PMT	Photomultiplier
SANDA	Supplying Accurate Nuclear Data for energy and non-energy Applications
TOF	Time-of-flight

List of figures

Figure 1. Schematic representation of the transmission set-up at the 50 m station of GELINA. 5

Figure 2. TOF-spectrum resulting from measurements with the ^{209}Bi 1.255 mm sample with Co and W black resonance filters in the beam and the accelerator operated at 400 Hz. The sample-in spectrum (C_{in}) is shown together with the total background (B_{in}) and its components defined in Eq. (3.3) 8

Figure 3. Comparison of the experimental and calculated transmission through the 1.255 mm thick Bi sample. The calculated transmissions are obtained with REFIT using the resonance parameters in JENDL-4.0 and ENDF/B-VIII.0, including a neutron energy adjustment to match the experimental result. 12

Figure 4. Comparison of the experimental and calculated transmission through the 4 mm thick Bi sample for energies between 50 keV and 100 keV. Figure shows the impact of the negative background cross section included in JENDL-4.0, which is not present in JENDL-5. 13

Figure 5. Comparison of experimental and calculated transmission through the 4 mm thick Bi sample for energies between 100 keV and 150 keV. 14

Figure 6. Comparison of evaluated cross sections and Harvey's experimental data [25] for energies between 150 keV and 200 keV. It shows that ENDF/B-VIII.0 evaluation follows Harvey's experimental points. 14

Figure 7. Comparison of evaluated cross sections and Harvey's experimental data for energies between 200 keV and 300 keV. It clearly shows that, above 200 keV, the JENDL-5 evaluation, like ENDF/B-VIII.0, follows Harvey's experimental data. 15

List of tables

Table 1. Characteristics of the bismuth samples used for the transmission measurements. The areal densities n_d were derived from the measured mass and area and the ^{209}Bi atomic mass reported in Ref. [11]..... 6

Table 2. Parameters for the analytical expressions of the background correction for the 1.255 mm sample-in and sample-out measurements. The parameters are derived from results of measurements with the Co and W black resonance filters in the beam and the accelerator operating at 400 Hz..... 9

Table 3. Parameters for the analytical expressions of the background correction for the 4 mm sample-in and sample-out measurements. The parameters are derived from results of measurements with the Co and W black resonance filters in the beam and the accelerator operating at 400 Hz..... 9

Annexes

Annex 1. Summary of the experiment information

Experimental description (ID 1)

1.	**Main Reference**		
2.	**Facility**	GELINA	[a]
3.	**Neutron production**		
	Neutron production beam	Electron	
	Nominal average beam energy	100 MeV	
	Nominal average current	50 μA	
	Repetition rate (pulses per second)	400 Hz	
	Pulse width	2 ns	
	Primary neutron production target	Mercury cooled depleted uranium	
	Target nominal neutron production intensity	3.4 x10^{13} s^{-1}	
4.	**Moderator**		
	Primary neutron source position in moderator	Above and below uranium target	
	Moderator material	2 water filled Be-containers around U-target	
	Moderator dimensions (internal)	2 x (14.6 cm x 21 cm x 3.9 cm)	
	Density (moderator material)	1 g/cm^3	
	Temperature (K)	Room temperature	
	Moderator-room decoupler (Cd, B, …)	None	
5.	**Other experimental details**		
	Measurement type	Transmission	
	Method (total energy, total absorption, …)	Good transmission geometry	[b]
	Flight Path length (m) (moderator centre-detector front face)	L = 47.669 (4) m	
	Flight path direction	9° with respect to normal of the moderator face viewing the flight path	
	Neutron beam dimensions at sample position	45 mm in diameter	
	Neutron beam profile	-	
	Overlap suppression	^{10}B overlap filter	
	Other fixed beam filters	Co, W, Pb	
6.	**Detector**		
	Type	Scintillator	
	Material	Li-glass	
	Surface Dimensions		
	Thickness (cm)	6.35 mm	
	Detector(s) position relative to neutron beam	In the beam	
	Detector(s) solid angle	-	
	Samples		
7.	Type (metal, powder, liquid, crystal)	Metal	
	Chemical composition	^{209}Bi (100 at %)	
	Sample composition (at/b)	3.4828 (4) x 10^{-3}	
	Temperature	20 °C	
	Sample mass (g)	62.214 (10)	
	Geometrical shape (cylinder, sphere, …)	Cylinder	
	Surface dimension (mm^2)	5147 (5)	

Nominal thickness (mm)	1.255	
Containment description	No container	
Data Reduction Procedure		[c][d]
8. Dead time correction	Done (< factor 1.2)	
Background subtraction	Black resonance technique	
Flux determination (reference reaction, …)	-	
Normalization	1.0000 (25)	
Detector efficiency	-	
Self-shielding	-	
Time-of-flight binning	Zone length bin width 6144 2 ns 6144 4 ns 4096 8 ns 4096 16 ns 3072 32 ns 2048 64 ns 2048 128 ns 2048 256 ns 2048 512 ns 1024 1024 ns	
Response function		
9. Initial pulse	Normal distribution, FWHM = 2 ns	
Target / moderator assembly	Numerical distribution from MC simulations	[e][f]
Detector	Analytical function defined in REFIT manual	[g]

Experimental description (ID 2)

1. Main Reference		
2. Facility	GELINA	[a]
3. Neutron production		
Neutron production beam	Electron	
Nominal average beam energy	100 MeV	
Nominal average current	50 μA	
Repetition rate (pulses per second)	400 Hz	
Pulse width	2 ns	
Primary neutron production target	Mercury cooled depleted uranium	
Target nominal neutron production intensity	3.4×10^{13} s^{-1}	
4. Moderator		
Primary neutron source position in moderator	Above and below uranium target	
Moderator material	2 water filled Be-containers around U-target	
Moderator dimensions (internal)	2 x (14.6 cm x 21 cm x 3.9 cm)	

	Density (moderator material)	1 g/cm^3	
	Temperature (K)	Room temperature	
	Moderator-room decoupler (Cd, B, …)	None	
5.	**Other experimental details**		
	Measurement type	Transmission	
	Method (total energy, total absorption, …)	Good transmission geometry	[b]
	Flight Path length (m) (moderator centre-detector front face)	L = 47.669 (4) m	
	Flight path direction	9° with respect to normal of the moderator face viewing the flight path	
	Neutron beam dimensions at sample position	45 mm in diameter	
	Neutron beam profile	-	
	Overlap suppression	^{10}B overlap filter	
	Other fixed beam filters	Na, Co, W, Pb	
6.	**Detector**		
	Type	Scintillator	
	Material	Li-glass	
	Surface Dimensions		
	Thickness (cm)	6.35 mm	
	Detector(s) position relative to neutron beam	In the beam	
	Detector(s) solid angle	-	
	Samples		
7.	Type (metal, powder, liquid, crystal)	Metal	
	Chemical composition	^{209}Bi (100 at %)	
	Sample composition (at/b)	1.1066 (11) x 10^{-2}	
	Temperature	20 °C	
	Sample mass (g)	201.865 (10)	
	Geometrical shape (cylinder, sphere, …)	Cylinder	
	Surface dimension (mm^2)	5256 (5)	
	Nominal thickness (mm)	4	
	Containment description	No container	
	Data Reduction Procedure		[c][d]
8.	Dead time correction	Done (< factor 1.2 below 100 keV)	
	Background subtraction	Black resonance technique	
	Flux determination (reference reaction, …)	-	
	Normalization	1.0000 (25)	
	Detector efficiency	-	
	Self-shielding	-	
	Time-of-flight binning	Zone length / bin width 12288 / 1 ns 12288 / 2 ns 8192 / 4 ns 8192 / 8 ns 6144 / 16 ns 4096 / 32 ns 4096 / 64 ns 4096 / 128 ns 4096 / 256 ns 2048 / 1024 ns	
	Response function		

9.	Initial pulse	Normal distribution, FWHM = 2 ns	
	Target / moderator assembly	Numerical distribution from MC simulations	[e][f]
	Detector	Analytical function defined in REFIT manual	[g]

Annex 2. Summary of data format

Column	Content	Unit	Comment
1	Energy	eV	Relativistic relation using a fixed flight path length (L = 47.67 m)
2	t_l	ns	Low bound
3	t_h	ns	High bound
4	T_{exp}		Transmission
5	Total Uncertainty		
6	Uncorrelated uncertainty		Uncorrelated uncertainty due to counting statistics
7	AGS-vector (K)		Background model uncertainty (u_K/K=3%)
8	AGS-vector (N)		Normalization (u_N/N = 0.25%)

Comments from the authors:

- The AGS concept was used to derive the experimental transmission

$$\mathrm{T_{exp}} = \mathrm{N}\frac{\mathrm{C_{in}} - \mathrm{KB_{in}}}{\mathrm{C_{out}} - \mathrm{KB_{out}}},$$

  and to propagate the uncertainties, both the uncorrelated due to counting statistics and the uncertainty due to the normalization and the background contributions.

- The quoted uncertainties are standard uncertainties at 1 standard deviation

Data example (ID 1)

E/ keV	t_l / ns	t_h / ns	T_{exp}	u_t	u_u	AGS K	AGS N
100.009	10898	10900	0.988497	0.013089	0.012854	-0.000010	0.002471
99.9730	10900	10902	0.975946	0.012888	0.012655	-0.000021	0.002440
…	…	…	…	…	…	…	…
0.80235	121664	121680	0.017640	0.003811	0.003169	-0.002116	0.000044
0.80214	121680	121696	0.018200	0.003951	0.003286	-0.002193	0.000046
…	…	…		…	…	…	…
0.30006	198944	198976	0.951560	0.011817	0.011575	-0.000079	0.002379
0.29997	198976	199008	0.963293	0.011876	0.011629	-0.000060	0.002408

Data example (ID 2)

E/ keV	t_l / ns	t_h / ns	T_{exp}	u_t	u_u	AGS K	AGS N
150.009	8899	8900	0.846318	0.023220	0.023123	-0.000102	0.002116
149.976	8900	8901	0.863010	0.024490	0.024395	-0.000098	0.002158
…	…	…	…	…	…	…	…
5.12083	48160	48164	0.460347	0.018777	0.018665	-0.001688	0.001151
5.11998	48164	48168	0.425198	0.017856	0.017735	-0.001784	0.001063
…	…	…		…	…	…	…
0.30004	198960	198976	0.898884	0.021338	0.021218	-0.000164	0.002247
0.29999	198976	198992	0.906043	0.021530	0.021411	-0.000154	0.002265

Annex references

[a] W. Mondelaers and P. Schillebeeckx, “GELINA, a neutron time-of-flight facility for neutron data measurements”, Notiziario Neutroni e Luce di Sincrotrone, 11 (2006) 19 – 25.

[b] P. Schillebeeckx, B. Becker,Y. Danon, K. Guber, H. Harada, J. Heyse, A.R. Junghans, S. Kopecky, C. Massimi, M.C. Moxon, N. Otuka, I. Sirakov and K. Volev, “Determination of resonance parameters and their covariances from neutron induced reaction cross section data”, Nuclear Data Sheets 113 (2012) 3054 – 3100.

[c] B. Becker, C. Bastian, J. Heyse, S. Kopecky and P. Schillebeeckx, “AGS – Analysis of Geel Spectra User's Manual”, NEA/DB/DOC(2014)4.

[d] B. Becker, C. Bastian, F. Emiliani, F. Gunsing, J. Heyse, K. Kauwenberghs, S. Kopecky, C. Lampoudis, C. Massimi, N. Otuka, P. Schillebeeckx and I. Sirakov, “Data reduction and uncertainty propagation of time-of-flight spectra with AGS”, J. of Instrumentation, 7 (2012) P11002 – 19.

[e] M. Flaska, A. Borella, D. Lathouwers, L.C. Mihailescu, W. Mondelaers, A.J.M. Plompen, H. van Dam and T.H.J.J. van der Hagen, “Modeling of the GELINA neutron target using coupled electron–photon–neutron transport with the MCNP4C3 code”, Nucl. Instr. Meth. A 531 (2004) 392–406.

[f] D. Ene, C. Borcea, S. Kopecky, W. Mondelaers, A. Negret and A.J.M. Plompen, “Global characterisation of the GELINA facility for high-resolution neutron time-of-light measurements by Monte Carlo simulations”, Nucl. Instr. Meth. A 618 (2010) 54 - 68.

[g] M.C. Moxon and J.B. Brisland, Technical Report AEA-INTEC-0630, AEA Technology (1991).

GETTING IN TOUCH WITH THE EU

In person

All over the European Union there are hundreds of Europe Direct centres. You can find the address of the centre nearest you online (european-union.europa.eu/contact-eu/meet-us_en).

On the phone or in writing

Europe Direct is a service that answers your questions about the European Union. You can contact this service:

— by freephone: 00 800 6 7 8 9 10 11 (certain operators may charge for these calls),

— at the following standard number: +32 22999696,

— via the following form: european-union.europa.eu/contact-eu/write-us_en.

FINDING INFORMATION ABOUT THE EU

Online

Information about the European Union in all the official languages of the EU is available on the Europa website (european-union.europa.eu).

EU publications

You can view or order EU publications at op.europa.eu/en/publications. Multiple copies of free publications can be obtained by contacting Europe Direct or your local documentation centre (european-union.europa.eu/contact-eu/meet-us_en).

EU law and related documents

For access to legal information from the EU, including all EU law since 1951 in all the official language versions, go to EUR-Lex (eur-lex.europa.eu).

Science for policy

The Joint Research Centre (JRC) provides independent, evidence-based knowledge and science, supporting EU policies to positively impact society

EU Science Hub
joint-research-centre.ec.europa.eu

Publications Office
of the European Union